Article

Not peer-reviewed version

Differential Gene Expression of Malaria Parasite in Response to Red Blood Cell-Specific Glycolytic Intermediate 2,3-Diphosphoglycerate (2,3-DPG)

Ana Balau , Daniel Sobral , Patrícia Abrantes , Inês Santos , Verónica Mixão , João Paulo Gomes , Sandra Antunes , Ana Paula Arez *

Posted Date: 13 November 2023

doi: 10.20944/preprints202311.0790.v1

Keywords: Plasmodium falciparum, infection, erythrocyte, pyruvate kinase deficiency, enzymopathy, 2,3-bisphosphoglycerate, transcriptome, Nanopore technology

Article

Differential Gene Expression of Malaria Parasite in Response to Red Blood Cell-Specific Glycolytic Intermediate 2,3-Diphosphoglycerate (2,3-DPG)

Ana Balau [1], Daniel Sobral [2], Patrícia Abrantes [1], Inês Santos [1], Verónica Mixão [2], João Paulo Gomes [2], Sandra Antunes [1] and Ana Paula Arez [1]*

[1] Global Health and Tropical Medicine, GHTM, Associate Laboratory in Translation and Innovation Towards Global Health, LA-REAL, Instituto de Higiene e Medicina Tropical, IHMT, Universidade NOVA de Lisboa, UNL, Lisbon, Portugal; a21001549@ihmt.unl.pt Ana Balau (A.B.); inesmariasantos2001@gmail.com Inês Santos (I.S.); patriciaabrantes@ihmt.unl.pt Patrícia Abrantes (P.A.); santunes@ihmt.unl.pt (S.A.)

[2] Genomics and Bioinformatics Unit, Department of Infectious Diseases, National Institute of Health Doutor Ricardo Jorge (INSA), Lisbon, Portugal; daniel.sobral@insa.min-saude.pt (D.S.); veronica.mixao@insa.min-saude.pt (V.M.); j.paulo.gomes@insa.min-saude.pt (J.P.G.)

* Correspondence: aparez@ihmt.unl.pt; Global Health and Tropical Medicine, GHTM, Associate Laboratory in Translation and Innovation To-wards Global Health, LA-REAL, Instituto de Higiene e Medicina Tropical, IHMT, Universidade NOVA de Lisboa, UNL, Rua da Junqueira, 100, 1349-008, Lisbon, Portugal; aparez@ihmt.unl.pt

Abstract: Innovative strategies to control malaria are urgently needed. Exploring the interplay between the *Plasmodium* sp. parasites and host red blood cells (RBC) offers opportunities for novel antimalarial interventions. Pyruvate kinase deficiency (PKD), characterized by heightened 2,3-diphosphoglycerate (2,3-DPG) concentration, has been associated with protection against malaria. Elevated 2,3-DPG levels, a specific mammalian metabolite, may hinder glycolysis, prompting us to hypothesize its potential contribution to PKD-mediated protection. We investigated the impact of the extracellular supplementation of 2,3-DPG on the *Plasmodium falciparum* intraerythrocytic developmental cycle *in vitro*. Results showed an inhibition of parasite growth, resulting from significantly less progeny from 2,3-DPG-treated parasites. We analyzed differential gene expression and the transcriptomic profile of *P. falciparum* trophozoites, from *in vitro* cultures submitted or not submitted to the action of 2,3-DPG, using Nanopore Sequencing Technology. The presence of 2,3-DPG in the culture medium was associated to a significant differential expression of 71 genes, mostly associated to GO terms nucleic acid binding, transcription, or monoatomic anion channel. Further, several genes related to the cell cycle control were downregulated in treated parasites. These findings suggest that the presence of this RBC-specific glycolytic metabolite impact the expression of genes transcribed during the parasite trophozoite stage and the number of merozoites released from individual schizonts, which supports the potential role of 2,3-DPG in the mechanism of protection against malaria by PKD.

Keywords: *Plasmodium falciparum*; infection; erythrocyte; pyruvate kinase deficiency; enzymopathy; 2,3-bisphosphoglycerate; transcriptome; nanopore technology

1. Introduction

Malaria remains one of the biggest world public health problems mainly affecting the poorest areas of the globe contributing to poverty and inequality [1]. The last World Malaria Report released in 2022, estimated that malaria has caused 247 million cases in 2021, from which approximately 593,000 resulted in deaths [2]. The economic impact of malaria is also vast as it includes costs related to health care, decreased productivity and investment [3]. The emergence and spread of resistance of mosquitoes to insecticides and parasites to antimalarial medicines, highlight the urgent necessity for new, efficacious malarial tools with minimal adverse effects [4].

Preprints (www.preprints.org) | NOT PEER-REVIEWED | Posted: 13 November 2023 doi:10.20944/preprints202311.0790.v1

Human genetic traits that provide protection against malaria have been selected and reach high frequencies in endemic areas [5]. Understanding the underlying mechanisms of this protection may unveil targets for new antimalarial approaches that could mimic the protective effects exhibited by naturally occurring Red Blood Cell (RBC) disorders [6]. Such tools may allow the delay of life-threatening parasite densities until clearance by immunity or by a co-delivered antimalarial drug. Besides, creating an unfavorable environment to the parasite by targeting host metabolic pathways also may help avoid drug resistance, as the therapeutic targets are not within, or produced by, the pathogen.

Pyruvate kinase deficiency (PKD) is an erythrocyte enzymopathy caused by mutations in the *pklr* gene and has been associated with resistance to malaria in murine models [7] and with reduced RBC infection in *Plasmodium falciparum* cultures [8]. Some of these mutations appear to have been positively selected in malaria-exposed populations [9–12] but the mechanisms underlying protection remain unknown.

Pyruvate kinase (PK) catalyzes the last step of glycolysis. PK-deficient RBC display decreased ATP and pyruvate production and increased concentrations of 2,3-Diphosphoglycerate (2,3-DPG) [13], synthesized on the RBC-specific Rapoport-Luebering shunt by biphosphoglycerate mutase (BPGM). The parasite depends on glucose to obtain energy during blood-stage development, and it holds a complete set of glycolytic enzymes that seem to differ biochemically and structurally from their host counterparts with exception of BPGM [14].

In a situation of PKD, host PK activity sharply decreases, and 2,3-DPG content rises. Therefore, since *Plasmodium* parasites do not metabolize 2,3-DPG, we hypothesized that 2,3-DPG accumulation could have detrimental consequences for it by rendering an intracellular environment unsuitable for parasite development and providing a potential mechanism of protection against infection.

Previous results showed that addition of 2,3-DPG to the *in vitro P. falciparum* culture medium significantly impaired the parasite's intraerythrocytic developmental cycle (IDC), the metabolic profile of 2,3-DPG treated infected cells became more similar to that of non-infected cells, and host cells have not been significantly affected. Also, parasites exposed to 2,3-DPG produced significantly less progeny, independently of the ATP level inside the cell [15,16]. Therefore, to confirm these preliminary results and understand the biological processes involved in this response, in this study we analyzed the differential gene expression and the transcriptomic profile of schizogonic *P. falciparum* trophozoites from *in vitro* cultures submitted or not submitted to the action of 2,3-DPG, using Nanopore Sequencing Technology.

2. Results

2.1. Effect of 2,3-DPG on the parasite intraerythrocytic development

2,3-DPG 8 mM is added to the culture medium for the first time at 0h. In cultures with an initial parasite density of 1% (Figure 1A), untreated cultures exhibited a significant increase in parasite density until 96h-108h, reaching a plateau of 10% and 11%. In contrast, cultures treated with 2,3-DPG maintained a consistent parasite density of around 1% throughout the entire assay. This result is consistent with previous findings and the same effect persists in cultures with increased volumes and higher initial parasite densities (Figure 1B).

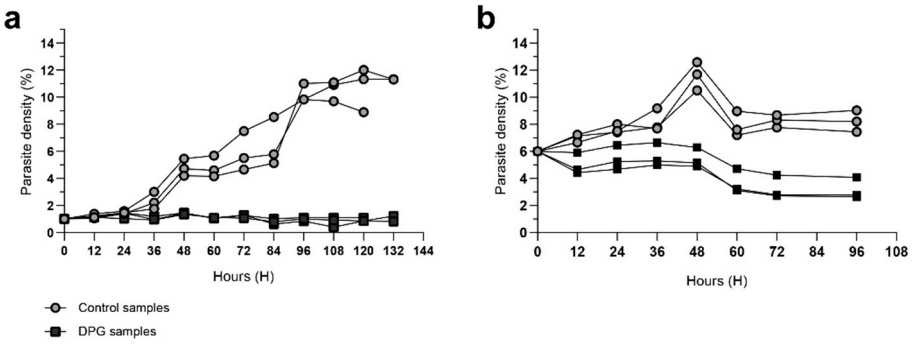

Preprints (www.preprints.org) | NOT PEER-REVIEWED | Posted: 13 November 2023 doi:10.20944/preprints202311.0790.v1

Figure 1. Parasite density (%) of *P. falciparum* 3D7 cultures untreated (control, light dots) or treated with 2,3-DPG 8 mM (dark squares). Assays were performed in triplicate for each condition using ring-stage synchronized cultures with initial parasite density of 1% (**a**) and 6% (**b**). First addition of 2,3-DPG 8 mM to the culture medium occurred at t = 0h; growth was monitored until lysis.

A morphological analysis of each stage of the parasite – ring, trophozoite, and schizont – was conducted using smears prepared every 12 hours between 46 and 48 hours of growth (Figure 2). The same trend was observed in cultures with both parasite density of 1% and 6%. No gametocytes were observed in either of the cultures. At the ring stage, no discernible morphological differences were noted between parasites from treated and untreated cultures. However, trophozoites from cultures treated with 2,3-DPG exhibited smaller size and appeared to possess higher cytoplasmic density. Similarly, differences were observed between treated and untreated mature schizonts, with those treated with 2,3-DPG displayed reduced size and seemed to yield fewer progeny (lower number of merozoites produced per mature schizont).

To validate the impact of the compound 2,3-DPG on the parasite's progeny, the count of merozoites produced by each mature schizont was performed every 12 hours between 46 and 48 hours of growth in each triplicate culture, totaling 100 schizonts per triplicate. The results derived from the merozoite count per schizont revealed a significant distinction between samples (p_value < 0.0001) (Figure 3). The number of merozoites generated by schizonts in cultures treated with 8 mM 2,3-DPG was notably lower compared to the number produced by schizonts in untreated cultures, applicable to both 1% and 6% parasite density cultures (Figure 3 A and B, respectively). The higher count of merozoites per mature schizont did not surpass 26 in cultures treated with 2,3-DPG. Conversely, in untreated cultures, the maximum count of merozoites per mature schizont reached 37.

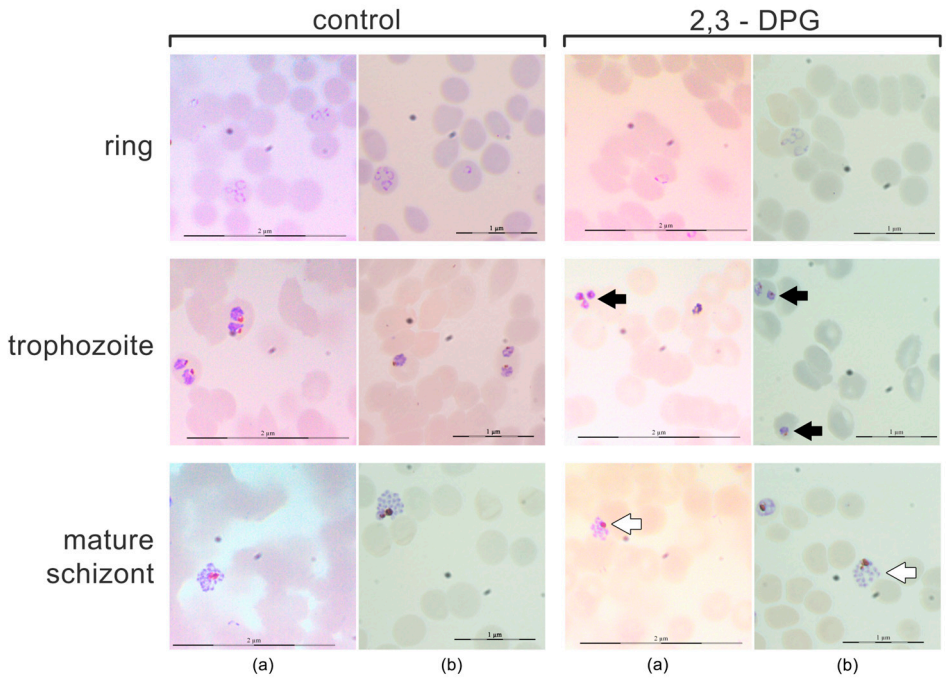

Figure 2. Morphological analysis of schizogonic stages – ring, trophozoite, and schizont, every 12 hours between 46 and 48 hours of growth. Giemsa-stained smears (optical microscope 1000x magnification) of *P. falciparum* 3D7 cultures in the absence (control) and presence of 2,3-DPG 8 mM (2,3-DPG) and 1% (a) and 6% (b) of parasite density. Less developed trophozoites (black arrows) and smaller schizonts and smaller progeny (lower number of merozoites) (white arrows) are visible in treated cultures.

Preprints (www.preprints.org) | NOT PEER-REVIEWED | Posted: 13 November 2023 doi:10.20944/preprints202311.0790.v1

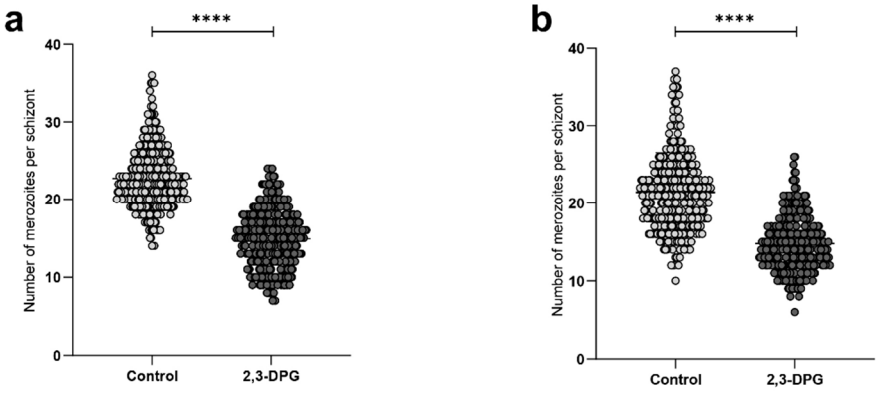

Figure 3. Number of merozoites produced by mature schizont in the absence (light dots) and presence of 2,3-DPG 8 mM (dark dots). 100 schizonts in each triplicate of treated and untreated cultures with 1% (A) and 6% (B) of parasite density were considered. **** p_value<0,0001. (**a**) Control: median = 22.00; mean = 22.73; SD = 4.07, and 2,3-DPG: median = 15.00; mean = 14.91; SD = 3.76. (**b**) Control: median = 21.00; mean = 21.42; SD = 5.12 and 2,3-DPG: median = 14.00; mean = 14.77; SD = 3.561.

2.2. Differentially expressed genes between treated and untreated cultures

For the assessment of differential gene expression between trophozoite stage parasites (30 hpi), exposed or not to 2,3-DPG, three replicates of each condition were used for RNA-Seq analysis. A total of 2,303,056 reads were obtained from which 69.1% passed the quality check, corresponding of 1,590,847 reads with a median read length of 1,422 bp, distributed by all libraries (barcodes). Details on the quality control (QC) of the sequencing data are provided in the Appendix A.

Sequencing reads passing all the QC steps were aligned to *P. falciparum* 3D7 reference genome. A total of 1,571,574 reads were mapped corresponding to 98.8% of total pass reads with an average accuracy of 91.52% and an average quality between 19.1 and 20.3 (statistics and quality for the alignment and mapping of the reads of each library are available on Appendix A).

Mapped reads across to all 14 chromosomes, apicoplast and mitochondrial genomes of *P. falciparum* are shown in Figure 4. Our results show that chromosomes 1, 5, 7 and 11 exhibited higher number of mapped reads, both for untreated (barcodes 01, 02 and 03) and treated samples (barcodes 04, 05 and 06). Most of these mapped reads correspond to RNA ribosomal genes (PF3D7_0112300, PF3D7_0112700, PF3D7_0531600, PF3D7_0531800, PF3D7_0532000, PF3D7_0725600, PF3D7_0725800, PF3D7_0726000, PF3D7_1148600, PF3D7_1148620 and PF3D7_1148640) or histones (PF3D7_1105000 and PF3D7_1105100). The same occurred regarding the apicoplast and mitochondrial genomes with the higher number of mapped reads corresponding to the genes PF3D7_API04900, PF3D7_API05700, PF3D7_API05900, PF3D7_API06700 and PF3D7_MIT02100.

Preprints (www.preprints.org) | NOT PEER-REVIEWED | Posted: 13 November 2023 doi:10.20944/preprints202311.0790.v1

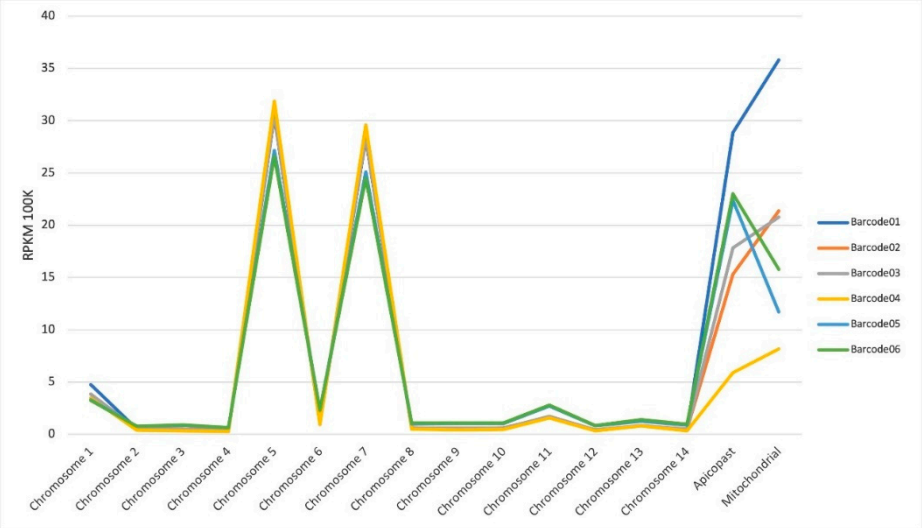

Figure 4. RPKM (Read Per Kilobase Mapped) per chromosome. Control (untreated samples: barcode01, barcode02, barcode03); DPG (treated samples: barcode04, barcode05, barcode06).

Principal component analysis (PCA) of the normalized counts for each barcoded revealed an effect of treatment, with barcodes 05 and 06 clustering together, as well as the three replicates of untreated cultures (barcodes 01, 02, and 03), with PC1 and PC2 explaining 47% and 22% of the variance, respectively (Figure 5A). However, barcode04 displayed distinct behavior from both groups, possibly due to technical issues during sample preparation. Subsequent analysis was conducted excluding reads originating from this library (Figure 5B). In this revised analysis, PC1 effectively separated treated samples from the untreated samples, accounting for 58% of the variance. Tabular files containing data with and without these reads are available as Supplementary Material – Table S1 and Table S2, respectively.

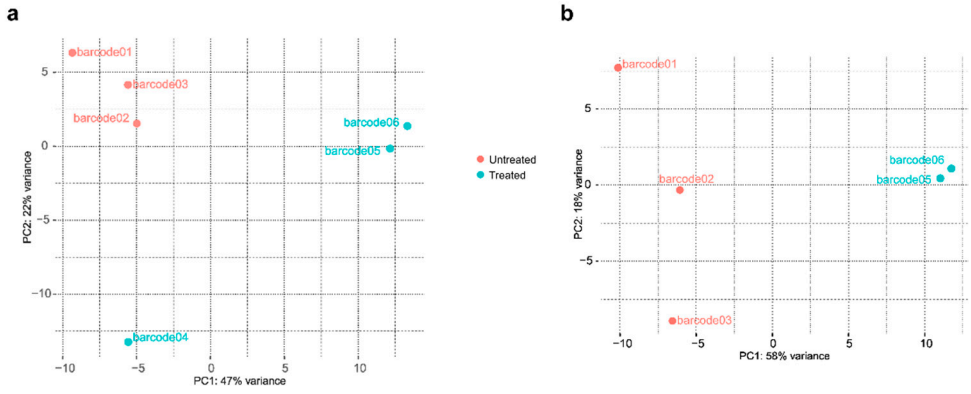

Figure 5. Principal component analysis (PCA) of the normalized counts for each barcoded library, with and without barcode04 (**a** and **b**, respectively).

A differential gene expression analysis between the two conditions was performed and revealed a total of 71 genes differentially expressed, two genes from the apicoplast genome (PF3D7_API05900 and PF3D7_API05700), six from the mitochondrial genome (PF3D7_MIT04000, PF3D7_MIT03200, PF3D7_MIT01400, PF3D7_MIT02300, PF3D7_MIT02100 and PF3D7_MIT01100) and 63 genes from the nuclear genome. From the total number of genes differentially expressed, three genes (4,2%) were upregulated (PF3D7_1302100, PF3D7_1239200 and PF3D7_1016900) and 68 genes (95,8%) were downregulated in the cultures submitted to 2,3-DPG (Figure 6 and Supplementary Table S3).

Preprints (www.preprints.org) | NOT PEER-REVIEWED | Posted: 13 November 2023 doi:10.20944/preprints202311.0790.v1

The heatmap plot displays the five barcoded samples on the X-axis that cluster based on treatment, and the 71 differentially expressed genes on the Y-axis. Replicates from treated samples (barcode05 and barcode06) show very similar levels of gene expression, and the same is observed for untreated samples (barcode01, barcode02, and barcode03) but substantial differences in gene expression levels are observed between the two conditions, which indicate that the presence of 8 mM 2,3-DPG in the culture medium caused a variation in the expression of genes transcribed during the trophozoite stage (30 hpi).

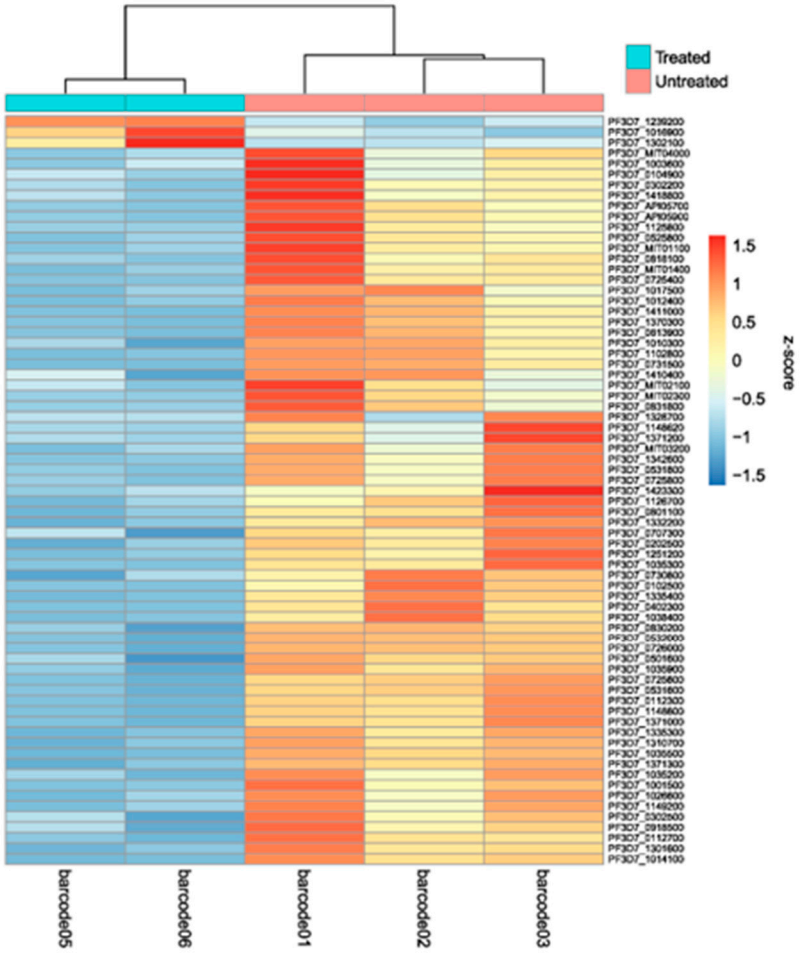

Figure 6. Heatmap of the differentially expressed genes between treated (barcodes 05 and 06) and untreated samples (barcodes 01, 02 and 03).

2.2.1. Gene Ontology enrichment analysis

To characterize the differentially expressed genes, we performed GO assignments to the three main GO categories: Molecular Function (MF), Biological process (BP) and Cellular component (CC). GO analysis showed that the most significant enriched GO terms were GO:0008201~heparin binding in the MF category, GO:0044409~entry into host in the BP category and GO term GO:0020008~rhoptry in the CC category (Table 1; gene products are detailed in Table S3).

Analyzing the metabolic pathways where the differentially expressed genes may be involved (Table S3), we observed that a total of 16 genes are annotated as coding proteins involved in cell cycle control, most of them downregulated. Among these, the PF3D7_1423300 (serine/threonine protein phosphatase 7) is annotated as a protein involved in steps during passage through prophase, the PF3D7_0525800 (inner membrane complex protein 1g, putative) is annotated as a protein predicted to be involved in cell cycle regulatory network and control of microtubule assembly. Also involved in cell cycle regulatory network is PF3D7_1038400 (gametocyte-specific protein) and PF3D7_1239200

 doi:10.20944/preprints202311.0790.v1

(AP2 domain transcription factor, putative), the latter being upregulated. The other 12 genes are annotated as functional orthologs of known cell cycle proteins in *Escherichia coli*.

Table 1. Summary of the most significant enriched GO terms according to the Gene Ontology enrichment analysis of the 71 genes differentially expressed in trophozoite stage parasites 30 hpi, exposed to 2,3-DPG.

GO category	GO term	Name	N. of genes	Study Freq.	Pop. Freq.	p-value	q-value
Molecular Function	GO:0008201	heparin binding	6	25%	0.68%	1.48E-9	8.11E-8
	GO:0005488	binding	23	96%	64%	2.70E-4	2.97E-3
	GO:0005253	monoatomic anion channel activity	2	8.3%	0.15%	3.15E-4	2.97E-3
	GO:0046812	host cell surface binding	6	25%	4.4%	4.36E-4	3.00E-3
Biological Process	GO:0044409	entry into host	11	50%	7.4%	7.87E-8	9.05E-6
Cellular Component	GO:0020008	rhoptry	7	18%	1.3%	3.22E-7	1.87E-5
	GO:1903561	extracellular vesicle	9	24%	2.9%	8.73E-7	2.53E-5
	GO:0016459	myosin complex	2	5.3%	0.10%	4.35E-4	4.2E-3
	GO:0020039	pellicle	2	5.3%	0.10%	4.35E-4	4.2E-3
	GO:0070258	inner membrane pellicle complex	5	13%	2.0%	8.80E-4	6.38E-3
	GO:0033643	host cell part	15	39%	18%	1.67E-3	9.89E-3
	GO:0009986	cell surface	6	16%	4.6%	7.31E-3	0.0353
	GO:0020009	microneme	3	7.9%	1.2%	9.88E-3	0.0441

Study Freq. – number of genes within the 71 genes differentially expressed associated with the GO term; Pop. Freq. – the number of genes in the entire background population (5,427 genes) associated with the GO term.

Two of the downregulated genes are related to the effect of hyperoxia on gene expression [PF3D7_1125800 (kelch domain-containing protein, putative), PF3D7_1017500 (myosin essential light chain ELC)].

Three genes have been found in previous studies to be differentially expressed in severe malaria [PF3D7_0613900 (myosin E, putative), PF3D7_0202500 (early transcribed membrane protein 2) and PF3D7_1102800 (early transcribed membrane protein 11.2)], significantly correlated with coma score [PF3D7_1335400 (reticulocyte binding protein 2 homologue a)] and 10 genes have been considered as candidate genes related to virulence.

The three protein-coding genes in the mitochondrial genome of *P. falciparum* (PF3D7_MIT01400 - cytochrome c oxidase subunit 3, PF3D7_MIT02300 - cytochrome b and PF3D7_MIT02100 - cytochrome c oxidase subunit 1) are shown to be downregulated in samples submitted to 2,3-DPG.

3. Discussion

Plasmodium has coevolved with humans for thousands of years, shaping both the parasite and its human host. Interactions between the host and infectious agents play a pivotal role in determining individual susceptibility and the morbidity experienced by infected individuals. Our research efforts have been dedicated to exploring the significance of PKD in conferring resistance against malaria.

We postulated that the accumulation of 2,3-DPG resulting from PKD might lead to an intracellular environment that is unfavorable for the *Plasmodium* parasite during its infection of RBC, thus contributing to the mechanism of protection against malaria. To investigate the interaction between the parasite and its host cell, we conducted an analysis using *in vitro P. falciparum* cultures

 doi:10.20944/preprints202311.0790.v1

with the addition of 2,3-DPG to the culture medium. Ideally, RBC from individuals with PKD should be employed; however, obtaining the necessary amounts of blood from these anemic individuals is challenging. Therefore, we validated the suitability of the model by observing a similar effect on the parasite, achieved either by introducing 2,3-DPG into the culture medium or inducing a PKD phenotype through enolase inhibition [15].

In the present study, we confirmed previous findings that when exposed to the influence of 2,3-DPG, parasites were unable to normally proceed to a new cycle of growth. In untreated cultures, an exponential rise in parasite density is evident, aligned with the 48-hour life cycle of the parasite. During this cycle, the schizont ruptures, releasing up to 32 merozoites [17], poised to invade new erythrocytes. However, this elevation in parasite density did not manifest in cultures treated with 2,3-DPG. The parasite could develop in the compound's presence between 0 and 24 hours, exhibiting identical parasite densities in untreated and treated cultures but it failed in progression by augmenting its parasite density in successive cycles. Earlier studies have also demonstrated that 2,3-DPG's impact on RBC deformability and membrane zeta potential was relatively minor, and these changes did not impede effective parasite re-invasion or egress. Moreover, cytotoxicity remained low, with no discernible alterations in ATP levels and no noticeable effect on the parasite when RBCs were subjected to 2,3-DPG treatment before infection (Carvalho et al., 2023; Morais et al., 2022). These findings strongly imply a direct influence of 2,3-DPG on the parasite. The inhibition of parasite growth is likely attributed to an impediment in parasite maturation, consequently yielding notably reduced progeny from parasites subjected to the treatment. Regulation of progeny number may arise due to nutrient exhaustion or stress factors [18,19]. However, it can also be impacted by intrinsic or extrinsic host factors, as replicated in the current study. Consequently, to delve into the biological mechanisms driving this phenomenon, we examined the impact of 2,3-DPG on parasite gene expression.

We analyzed the differential gene expression between *P. falciparum* trophozoites from *in vitro* cultures submitted or not submitted to the action of 2,3-DPG. At present, only some few malaria studies based on nanopore technology have been reported addressing DNA sequencing diagnostics and genotyping [20–22] and de novo assembly of *Plasmodium* sp. genomes [23,24]. To our knowledge none has addressed differential expression under different environmental conditions.

The presence of 2,3-DPG in the culture medium caused a clear effect on the expression of genes transcribed during the trophozoite stage at 30 hpi, which is the approximate timepoint when the first round of DNA replication begins in *P. falciparum* asexual blood stages [25]. The parasite undergoes then several rounds of DNA replication and nuclear division that are not directly followed by cytokinesis, resulting in multinucleated cells. The number of generated nuclei in *Plasmodium* directly predicts the number of progeny emerging from an infected cell [19]. Our results have shown that several genes differentially expressed, most of them downregulated, are related to cell cycle proteins that control the progression of a eukaryotic cell through the various phases of the cell cycle, which may explain the observation of reduced progeny from treated parasites.

Apart from the lower progeny, morphological analysis revealed less developed trophozoites and smaller schizonts when parasites were treated with 2,3-DPG. In the infected RBC, the glucose uptake and lactate production increase almost 100-fold [26] and a disruption of the parasite glycolytic chain could affect parasite development or proliferation [27]. At least at the transcription level no impairment of parasite glycolysis occurred since we could not detect significant differences in expression of the genes that code for key enzymes of glycolysis such as hexokinase (PF3D7_0624000), phosphofructokinase (PF3D7_1128300), pyruvate kinase (PF3D7_0626800), and phosphoglycerate kinase (PF3D7_0922500) in untreated and treated samples. However, the three protein-coding genes in the mitochondrial genome were downregulated and this may impact the energy production in the parasite's mitochondria, affecting its survival and replication. Furthermore, an effect related to the effect of hyperoxia on gene expression was observed. It is known that hyperoxia may influence the parasite metabolic pathways and affect its growth and reproduction [28,29]. 2,3-DPG is an allosteric regulator of oxygen affinity to hemoglobin and increased 2,3-DPG levels inside the cell would result

 doi:10.20944/preprints202311.0790.v1

in decreased O2-bound hemoglobin, and a variation in O_2 pressure leading to direct exposure of parasite to hyperoxia.

The transcriptionally active genome varies during the IDC [30]. Present analysis focused the trophozoite stage (30 hpi), the most metabolically and transcriptionally active asexual stage [31]. We observed enrichment in GO terms associated with nucleic acid binding, transcription, or monoatomic anion channel activity, consistent with biological processes that are known to occur at this stage, such as translation and DNA replication and an active metabolism [31,32]. However, strong enrichment was also observed in processes related to the entry into host cell, rhoptry and microneme, which reason is not clear. In addition to these processes are predominant in schizonts, we have not observed before any differences in invasion of RBC by treated or untreated parasites [15,16].

Although the effect of treatment with 2,3-DPG had been clearly shown, this study has some limitations. Poly(A) selection may inconsistently bias mRNA expression [33] and the low number of replicates per condition and high variability within replicates, especially regarding the untreated samples, prevent definitive conclusions. We consider the present study as preliminary, but it has an important exploratory value as a pilot to further studies with a larger number of replicates to complement the work described in this paper. However, we show that the analysis based on ONT serves as an effective approach to detect the effect of different treatments on parasites. Although the major limitation of nanopore sequencing is its lower read accuracy when compared with short-read technologies, the advantages of long reads outweigh the low-read accuracy [34]. ONT long-read sequencing provides real-time, amplification-free, single molecule sequencing of cDNAs that enables recovery of full-length transcripts without the need for an assembly step and so quantifying the expression of genes can be done by simple counting of the assigned reads [35–37].

To have the comprehensive picture of the effect of 2,3-DPG or the PKD on the *Plasmodium* parasite, future studies should address the full IDC, validate confirmed differential expressed genes by quantitative RT-PCR and perform subsequent functional analysis. Also, the possibility of reading full-length transcripts and thus efficiently identify RNA molecules and transcript isoforms, including transcript length and splice isoforms opens up perspectives for the analysis of regulatory roles and splicing events triggered by the exposure of the parasite to different intracellular conditions [36,38,39].

4. Materials and Methods

4.1. Blood donors

Healthy-type 0 RBC were collected from adult volunteer donors (n = 5). Blood variants of genes associated with malaria protection that could influence parasite growth were ruled out through the molecular diagnosis of the polymorphisms most common in Portugal, namely of genes HBB—haemoglobin subunit beta, pklr—pyruvate kinase, liver and red blood cell, and g6pd - —glucose-6-phosphate dehydrogenase, as described by Morais et al. (2022). Every donor was wild type for all studied genes.

All donors were clearly informed that participation in the study was voluntary and were made aware of the objectives of the work. An informed consent form was signed by each participant before blood collection, and a numerical code was assigned to each donor to maintain confidentiality.

4.2. Plasmodium falciparum in vitro cultures

Plasmodium falciparum 3D7 parasites (BEI Resources MRA-102) were maintained in RBC at 5% hematocrit at 37 ºC in a wet atmosphere with 5% CO_2, accompanied by daily complete Gibco Roswell Park Memorial Institute 1640 Medium (cRPMI) changes [40]. Parasite growth was monitored daily through estimation of the parasite density (percentage of infected cells) in 20% Giemsa-stained (Giemsa's Azur-eosin–methylene blue, Sigma-Aldrich, Darmstadt, Germany) thin blood smears.

All assays have been performed after synchronization of cultures with 5% (w/v) sorbitol (Sigma-Aldrich), following an adapted protocol [41] and initiated with ring-stage forms 6-8 hours post-invasion (hpi).

 doi:10.20944/preprints202311.0790.v1

4.3. Effect of 2,3-DPG on the parasite intraerythrocytic development

To study the effect of the compound on parasites, solutions of 2,3-diphospho-D-glyceric acid pentasodium salt (Sigma-Aldrich, Darmstadt, Germany) 1.33 M were prepared in ultrapure water, from which intermediate dilutions were done with cRPMI. The synthetic compound 2,3-DPG was added to the culture medium at a concentration of 8 mM as it has previously been shown that this concentration impairs the *in vitro* parasite growth cycle by 50% after 48 hours of treatment [15].

A culture of ring-stage parasitized RBC was divided into 12 new cultures with 5% hematocrit and 1% and 6% of parasite density (six each). Six cultures were added with 8mM 2,3-DPG and the remaining six cultures were not subjected to the treatment. Daily changes of medium, supplemented or not with 2,3-DPG, were performed and no RBCs were added to the cultures throughout the assay.

After 12 hours of growth, 6 µl of each culture was collected in triplicate into a 96-well flat bottom plate with lid and the parasite density was read on a flow cytometer (CytoFLEX, Beckman Coulter). 100 µl of 0.5X SYBR Green solution in PBS and 94 µl of RPMI medium were added to each well and plates incubated for 45 minutes at 37 ºC and 5% CO_2. After centrifugation, cells were washed and resuspended in the same volume of PBS. Three independent assays were performed in triplicate. This procedure was repeated every 12 hours until the lysis of the cultures. Circa 1,000 RBC were analyzed per well, and the parasite density was calculated using FlowJo v. 10 software (Tree Start Inc., Ashland, OR, USA).

Thin blood smears were made every 12 hours between 46 and 48h of growth and observed by light microscopy (Olympus BX40, 1000x) for a morphological analysis of parasites; images were captured using the ProgRes Capture Pro 2.1 program. In the same smears, the number of resulting merozoites from nuclear division in mature schizonts (segmenter stage) have been counted. In total, 100 mature schizonts per replicate, from treated and untreated cultures, with both 1% and 6% of parasite density, were considered.

4.4. RNA preparation

To obtain a minimum RNA amount of 100 ng, recommended for cDNA library preparation, it would be necessary to elevate the parasite density. Therefore, total parasite RNA was obtained from new six synchronized cultures of *P. falciparum* with 5% hematocrit and parasite density ranging from 7.5% to 11%. 8mM 2,3-DPG was added to three cultures and the remaining three cultures were not subjected to the treatment. Cultures were maintained in standard conditions and the parasite was isolated at 30h hours of the first growth cycle, corresponding to the stage of trophozoite (confirmed by optical microscopy). From each culture, the parasite was isolated from 300 µL of parasitized RBC with 1 mL of 0.05% saponin (Sigma-Aldrich) and incubated on ice for five minutes according to the procedure described by Lee et al. [36].

Afterwards, total parasite RNA was extracted from the three replicates of both treated and untreated synchronized cultures of *P. falciparum* at the trophozoite stage (30 hpi), using NZYol reagent and processed according to the manufacturer's instruction (Nzytech). Integrity and quantity of RNA were determined using a Qubit 4.0 fluorometer (Invitrogen) and a NanoDrop 1000 spectrophotometer (ThermoFisher).

4.5. cDNA library construction and transcriptome sequencing

For the construction of cDNA libraries, Direct cDNA Sequencing kits (SQK-DCS109) and Native Barcoding Expansion 1-12 (EXP-NBD104) from Oxford Nanopore Technology (ONT) were used according to the manufacturer´s protocol. The latter allows the multiplex and simultaneous analysis of up to 12 different samples subjected to different treatments.

cDNA libraries were constructed from the triplicate cultures for each condition (supplemented or not with 2,3-DPG). Briefly, the reverse transcription was followed by enzymatic digestion of the RNA template and synthesis of the second strand of cDNA. At the end, the poly-A ends were repaired, and the barcode sequences and the sequencing adapters were ligated. Six barcodes were

 doi:10.20944/preprints202311.0790.v1

ligated to each sample (untreated samples: barcode01, barcode02 and barcode03; treated samples: barcode04, barcode05 and barcode06).

Barcoded libraries were quantified using a Qubit fluorometer, by Qubit 1x dsDNA HS assay kit (Invitrogen). Barcoded libraries were pooled together, loaded on a MinION R9.4.1 flow cell (ONT) and sequenced at MinION Mk1C (ONT) for 24 hours (until the number of viable nanopores significantly reduced). Sequences were obtained through the MinKNOW software v1.10 onboard MinION and only "pass reads" were used in the analyses.

4.6. Analysis of gene expression

Base calling was performed by Guppy v5.1.13 software from MinKNOW v4.5.4 and FastQ files were generated with reads separated per barcode in folders. Each barcode folder was concatenated in a simple file with a Unix command line and quality was checked with pycoQC v2.5.2 and FastQC v0.74 on the platform Galaxy and Fastq Control Experiment v3.7.3 from Epi2Me Desktop Agent (ONT).

The absence of barcode sequences was verified in each concatenated file using a Unix command line, through the command gunzip -c "name_of_the_file".fastq.gz | grep 0: "barcode_sequencing" | wc -1. Minimap2 v2.24 was used to align and map the reads to the P. falciparum 3D7 reference genome (source version GCA_000002765.3), downloaded from PlasmoDB r.63. SAMtools stats v2.0.4 and Artemis Software Sanger r.18.2.0 were used to check mapping quality. The number of mapped reads to each of the 14 chromosomes of P. falciparum were checked by Samtools IdxStats v2.0.4 and MultiQC v1.11. The program featureCounts v2.0.3 was used to count mapped reads assigned to each gene match in an annotation file, after selecting the "Long reads" option. The annotation file was obtained from PlasmoDB r.63. Differences on gene expression were analyzed through DESeq2 v2.11.40.7. Genes were considered differentially expressed under the effect of 2,3-DPG (treated/untreated) when a logarithmic (base 2) difference in expression is different than zero and a corrected p-value of less than 5% ($p<0.05$) were obtained [$\log2(FC) > 0$ indicates upregulation and $\log2(FC) < 0$ indicates downregulation of genes]. Graphical representation of differentially expressed genes was performed by Heatmap2 (v3.1.3), as described in the Reference-based RNA-Seq data analysis workflow [42]. Gene Ontology (GO) enrichment analysis was carried out by genes sets based on corrected p-value<0.05 with GO enrichment v2.0.0.

4.7. Statistical analysis

Statistical analysis related with the effect of 2,3-DPG on the parasite was performed using GraphPad Prism program v. 8 (GraphPad Software). Comparison of merozoite count per mature schizont was performed by the unpaired T-student method. The statistical significance level was set at $p<0.05$.

5. Conclusions

In this study, we confirmed previous results that addition of 2,3-DPG to the *in vitro P. falciparum* culture medium significantly impaired the parasite's IDC, due to a significant reduction in the progeny produced by treated parasites and we show that this may be due to a downregulation of several genes related to the cell cycle control.

The number of merozoites released from an individual schizont is a key-determining factor for multiplication rate of the parasite. Lower multiplication rates would benefit the majority of individuals early in infection, due to delayed onset of high parasite densities and slower progression to anemia, potentially preventing the development of severe malaria early in infection. Host mechanisms such as systemic host inflammation [43] or enzymopathies such as PKD, and associated metabolites may trigger transcriptional alterations in circulating blood-stage *Plasmodium* trophozoites and may impair parasite maturation *in vivo*. Research must continue to assess whether these mechanisms may provide adjunct tools to enhance the effectiveness of existing antimalarial drugs.

Supplementary Materials: The following supporting information can be downloaded at the website of this paper posted on Preprints.org. Table S1: Identification and statistics of the differentially expressed genes with data from barcode 04, Table S2: Identification and statistics of the differentially expressed genes without data from barcode 04, Table S3: GO enrichment analysis of differentially expressed genes.

Author Contributions: Conceptualization, S.A. and A.P.A.; methodology, S.A. and A.P.A.; formal analysis, A.B., D.S. and P.A.; investigation, A.B. and I.S.; writing—original draft preparation, A.B. and A.P.A.; writing—review and editing, A.P.A., D.S., V.M., J.P.G. and S.A.; supervision, S.A. and A.P.A.; project administration, A.P.A..; funding acquisition, A.P.A. All authors have read and agreed to the published version of the manuscript.

Funding: This research was funded by Fundação para a Ciência e a Tecnologia—Ministério da Ciência, Tecnologia e Ensino Superior (FCT-MCTES, Portugal; https://www.fct.pt/en/ (accessed on 2 August 2023)) projects PTDC_BIA-CEL_28456_2017, GHTM—UID/04413/2020 (https://ghtm.ihmt.unl.pt/, accessed on 2 August 2023) and LA-REAL LA/P/0117/2020.

Institutional Review Board Statement: The study was conducted in accordance with the Declaration of Helsinki and approved by the Ethics Committee of the Institute of Hygiene and Tropical Medicine, Lisbon, Portugal (as part of project with reference PTDC_BIA-CEL_28456_2017, ethical review n. 16.18).

Informed Consent Statement: Informed consent was obtained from all subjects involved in the study.

Data Availability Statement: The RNA sequencing data presented in this study are openly available in the Sequence Read Archive (SRA) of the National Center for Biotechnology Information (NCBI) of the National Institute of Health (NIH), USA, with accession number PRJNA1036731. Additional resulting data sets are included in the article as well as the supplementary files.

Acknowledgments: We would like to thank all blood donors and Ana Reis from the Institute of Hygiene and Tropical Medicine, Lisbon, Portugal, for collecting the blood samples.

Conflicts of Interest: The authors declare no conflict of interest. The funders had no role in the design of the study; in the collection, analyses, or interpretation of the data; in the writing of the manuscript or in the decision to publish the results.

Appendix A

A.1. Transcriptome sequencing analysis – quality control

A.1.1. RNA quality and cDNA libraries sequencing

The RNA concentrations ranged from 60.4 to 412.0 ng/μL in a final volume of 20 μL, with integrity values between 5.5 and 10.0. The purity, as assessed by the A260/A280 ratio, varied within an optimal range of 2.04 and 2.22. Final concentration of barcoded libraries was 7.14 ng/μL, corresponding to 85.68 ng of cDNA in a final volume of 12 μL.

Barcoded libraries were pooled together and sequenced on a MinION R9.4.1 flow cell at a MinION Mk1C device for 24 hours, yielding a total of approximately 2.3 million reads. Quality control confirmed the absence of barcode sequences. According to pycoQC software, sequences with a Qscore equal to or higher than 7 are considered as 'pass' reads. From the total number of reads analyzed (2,303,056 reads), 69.1% of reads passed FastQ quality check, corresponding of 1,590,847 reads with a median read length of 1,422 bp, distributed by all libraries (712,209 were unclassified or poor-quality sequences). Number of pass reads and sequence length per barcode are represented in Table A1.

The base-called reads' PHRED quality plot from PycoQC indicates that most reads have Qscores between 8 and 12, is centered around 8.44 and showed a median PHRED score of 9.57. The distribution of pass reads length shows that the minimum read length is around 200 bp, while the maximum read length reaches approximately 10,000 bp. The plot displays a dispersed distribution, and about 10% of pass reads exceed 3 kb in length. (Figure A1).

A.1.2. Alignment and mapping of reads against the 3D7 reference genome

Reads from all the libraries were aligned and mapped against the *P. falciparum* 3D7 reference genome. Statistics for the mapped reads, including the proportion of mismatches per mapped bases (error rate) and mapping quality, are presented in Table A2. A total of 1,571,574 reads were mapped

Preprints (www.preprints.org) | NOT PEER-REVIEWED | Posted: 13 November 2023 doi:10.20944/preprints202311.0790.v1

corresponding to 98.8% of total pass reads with an average accuracy of 91.52% and an average quality between 19.1 and 20.3.

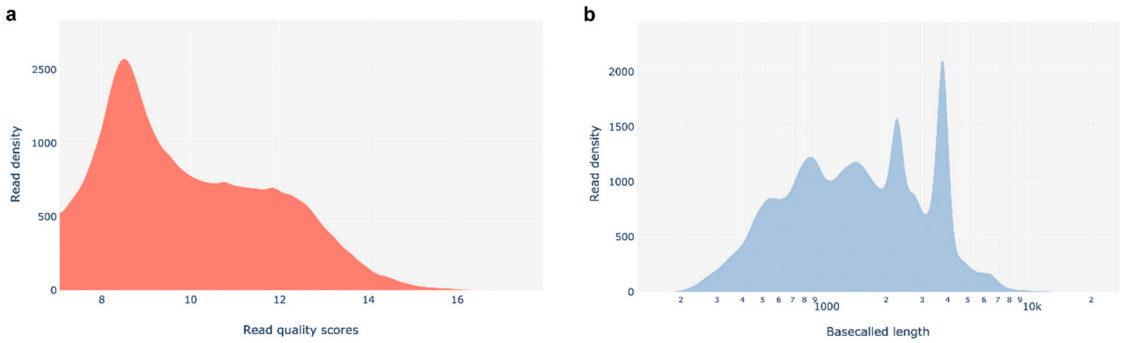

Figure A1. Summary of the quality control of sequencing data (according to PycoQC). (**a**) Basecalled reads PHRED quality - distribution of the Qscores for each read giving a global quality score for each read. (**b**) Basecalled reads length - minimum read length around 200 bp and a maximum read length around 10,000 bp.

Table A1. Number of pass reads and sequence length per barcode.

	Control (untreated samples)			DPG (treated samples)		
	Barcode01	**Barcode02**	**Barcode03**	**Barcode04**	**Barcode05**	**Barcode06**
Number of Pass reads (%)	124,497 (7.83%)	262,680 (16.51%)	165,905 (10.43%	246,274 (15.48%)	225,089 (14.15%)	566,402 (35.60%)
	553,082 (34.77%)			1,037,765 (65.23%)		
Total number of bases (Mbp)	201.3	423.2	270.9	537.4	414.6	1000.0
Sequence length	128-46,300	117-23,141	110-21,960	104-29,694	141-29,207	127-30,804

Table A2. Statistics and quality for the alignment and mapping of the reads of each library against the P. falciparum 3D7 reference genome (source version GCA_000002765.3).

		Total N. of Sequences	Mapped Reads	Unmapped Reads	Error rate	Average length	Average quality
Control (untreated samples)	**Barcode01**	124,497	122,745 (98.6%)	1,752 (1.4%)	9.63e-2	1,617	19.2
	Barcode02	262,680	257,908 (98.2%)	4,772 (1.8%)	9.65e-2	1,611	19.1
	Barcode03	165,905	163,915 (98.8%)	1,990 (1.2%)	9.63e-2	1,633	19.3
DPG (treated samples)	**Barcode04**	246,274	242,957 (98.7%)	3,317 (1.3%)	9.49e-2	2,182	19.1
	Barcode05	225,089	222,821 (99%)	2,268 (1%)	1.04e-1	1,842	19.8
	Barcode06	566,402	561,228 (99.1%)	5,174 (0.9%)	1.07e-1	1,826	20.3

References

1. Prudêncio, M.; Costa, J.C. Research Funding after COVID-19. *Nat. Microbiol.* **2020**, *5*, 986–986, doi:10.1038/s41564-020-0768-z.
2. World Health Organization *World Malaria Report 2022*; World Health Organization: Geneva, 2022; ISBN ISBN 978-92-4-006489-8.

3. Andrade, M.V.; Noronha, K.; Diniz, B.P.C.; Guedes, G.; Carvalho, L.R.; Silva, V.A.; Calazans, J.A.; Santos, A.S.; Silva, D.N.; Castro, M.C. The Economic Burden of Malaria: A Systematic Review. *Malar. J.* **2022**, *21*, 283, doi:10.1186/s12936-022-04303-6.
4. Mathews, E.S.; Odom John, A.R. Tackling Resistance: Emerging Antimalarials and New Parasite Targets in the Era of Elimination. *F1000Research* **2018**, *7*, 1170, doi:10.12688/f1000research.14874.1.
5. Lelliott, P.M.; McMorran, B.J.; Foote, S.J.; Burgio, G. The Influence of Host Genetics on Erythrocytes and Malaria Infection: Is There Therapeutic Potential? *Malar. J.* **2015**, *14*, 289, doi:10.1186/s12936-015-0809-x.
6. Zumla, A.; Rao, M.; Wallis, R.S.; Kaufmann, S.H.E.; Rustomjee, R.; Mwaba, P.; Vilaplana, C.; Yeboah-Manu, D.; Chakaya, J.; Ippolito, G.; et al. Host-Directed Therapies for Infectious Diseases: Current Status, Recent Progress, and Future Prospects. *Lancet Infect. Dis.* **2016**, *16*, e47–e63, doi:10.1016/S1473-3099(16)00078-5.
7. Min-Oo, G.; Fortin, A.; Tam, M.-F.; Nantel, A.; Stevenson, M.M.; Gros, P. Pyruvate Kinase Deficiency in Mice Protects against Malaria. *Nat. Genet.* **2003**, *35*, 357–362, doi:10.1038/ng1260.
8. Ayi, K.; Liles, W.C.; Gros, P.; Kain, K.C. Adenosine Triphosphate Depletion of Erythrocytes Simulates the Phenotype Associated with Pyruvate Kinase Deficiency and Confers Protection against *Plasmodium Falciparum* In Vitro. *J. Infect. Dis.* **2009**, *200*, 1289–1299, doi:10.1086/605843.
9. Alves, J.; Machado, P.; Silva, J.; Gonçalves, N.; Ribeiro, L.; Faustino, P.; do Rosário, V.E.; Manco, L.; Gusmão, L.; Amorim, A.; et al. Analysis of Malaria Associated Genetic Traits in Cabo Verde, a Melting Pot of European and Sub Saharan Settlers. *Blood Cells Mol Dis* **2010**, *44*, 62–68, doi:10.1016/j.bcmd.2009.09.008.
10. Machado, P.; Pereira, R.; Rocha, A.M.; Manco, L.; Fernandes, N.; Miranda, J.; Ribeiro, L.; Do Rosário, V.E.; Amorim, A.; Gusmão, L.; et al. Malaria: Looking for Selection Signatures in the Human PKLR Gene Region. *Br. J. Haematol.* **2010**, *149*, 775–784, doi:10.1111/j.1365-2141.2010.08165.x.
11. Machado, P.; Manco, L.; Gomes, C.; Mendes, C.; Fernandes, N.; Salomé, G.; Sitoe, L.; Chibute, S.; Langa, J.; Ribeiro, L.; et al. Pyruvate Kinase Deficiency in Sub-Saharan Africa: Identification of a Highly Frequent Missense Mutation (G829A;Glu277Lys) and Association with Malaria. *PLOS ONE* **2012**, *7*, e47071, doi:10.1371/journal.pone.0047071.
12. van Bruggen, R.; Gualtieri, C.; Iliescu, A.; Louicharoen Cheepsunthorn, C.; Mungkalasut, P.; Trape, J.-F.; Modiano, D.; Sodiomon Sirima, B.; Singhasivanon, P.; Lathrop, M.; et al. Modulation of Malaria Phenotypes by Pyruvate Kinase (PKLR) Variants in a Thai Population. *PLOS ONE* **2015**, *10*, e0144555, doi:10.1371/journal.pone.0144555.
13. van Wijk, R.; van Solinge, W.W. The Energy-Less Red Blood Cell Is Lost: Erythrocyte Enzyme Abnormalities of Glycolysis. *Blood* **2005**, *106*, 4034–4042, doi:10.1182/blood-2005-04-1622.
14. Roth, E. Plasmodium Falciparum Carbohydrate Metabolism: A Connection between Host Cell and Parasite. *Blood Cells* **1990**, *16*, 453–460; discussion 461-466.
15. Morais, I.; Medeiros, M.M.; Carvalho, M.; Morello, J.; Teixeira, S.M.; Maciel, S.; Nhantumbo, J.; Balau, A.; Rosa, M.T.G.; Nogueira, F.; et al. Synthetic Red Blood Cell-Specific Glycolytic Intermediate 2,3-Diphosphoglycerate (2,3-DPG) Inhibits Plasmodium Falciparum Development In Vitro. *Front. Cell. Infect. Microbiol.* **2022**, *12*, doi:10.3389/fcimb.2022.840968.
16. Carvalho, M.; Medeiros, M.M.; Morais, I.; Lopes, C.S.; Balau, A.; Santos, N.C.; Carvalho, F.A.; Arez, A.P. 2,3-Diphosphoglycerate and the Protective Effect of Pyruvate Kinase Deficiency against Malaria Infection—Exploring the Role of the Red Blood Cell Membrane. *Int. J. Mol. Sci.* **2023**, *24*, 1336, doi:10.3390/ijms24021336.
17. Venugopal, K.; Hentzschel, F.; Valkiūnas, G.; Marti, M. Plasmodium Asexual Growth and Sexual Development in the Haematopoietic Niche of the Host. *Nat. Rev. Microbiol.* **2020**, *18*, 177–189, doi:10.1038/s41579-019-0306-2.
18. Mancio-Silva, L.; Slavic, K.; Grilo Ruivo, M.T.; Grosso, A.R.; Modrzynska, K.K.; Vera, I.M.; Sales-Dias, J.; Gomes, A.R.; MacPherson, C.R.; Crozet, P.; et al. Nutrient Sensing Modulates Malaria Parasite Virulence. *Nature* **2017**, *547*, 213–216, doi:10.1038/nature23009.
19. Simon, C.S.; Stürmer, V.S.; Guizetti, J. How Many Is Enough? - Challenges of Multinucleated Cell Division in Malaria Parasites. *Front. Cell. Infect. Microbiol.* **2021**, *11*, 658616, doi:10.3389/fcimb.2021.658616.
20. Hamilton, W.L.; Ishengoma, D.S.; Parr, J.B.; Bridges, D.J.; Barry, A.E. Nanopore Sequencing for Malaria Molecular Surveillance: Opportunities and Challenges. *Trends Parasitol.* **2023**, S1471492223002350, doi:10.1016/j.pt.2023.09.014.
21. Imai, K.; Tarumoto, N.; Runtuwene, L.R.; Sakai, J.; Hayashida, K.; Eshita, Y.; Maeda, R.; Tuda, J.; Ohno, H.; Murakami, T.; et al. An Innovative Diagnostic Technology for the Codon Mutation C580Y in Kelch13 of Plasmodium Falciparum with MinION Nanopore Sequencer. *Malar. J.* **2018**, *17*, 217, doi:10.1186/s12936-018-2362-x.
22. Runtuwene, L.R.; Tuda, J.S.B.; Mongan, A.E.; Makalowski, W.; Frith, M.C.; Imwong, M.; Srisutham, S.; Nguyen Thi, L.A.; Tuan, N.N.; Eshita, Y.; et al. Nanopore Sequencing of Drug-Resistance-Associated Genes in Malaria Parasites, Plasmodium Falciparum. *Sci. Rep.* **2018**, *8*, 8286, doi:10.1038/s41598-018-26334-3.

23. Godin, M.J.; Sebastian, A.; Albert, I.; Lindner, S.E. Long-Read Genome Assembly and Gene Model Annotations for the Rodent Malaria Parasite Plasmodium Yoelii 17XNL. *J. Biol. Chem.* **2023**, *299*, 104871, doi:10.1016/j.jbc.2023.104871.
24. Oresegun, D.R.; Thorpe, P.; Benavente, E.D.; Campino, S.; Muh, F.; Moon, R.W.; Clark, T.G.; Cox-Singh, J. De Novo Assembly of Plasmodium Knowlesi Genomes From Clinical Samples Explains the Counterintuitive Intrachromosomal Organization of Variant SICAvar and Kir Multiple Gene Family Members. *Front. Genet.* **2022**, *13*, 855052, doi:10.3389/fgene.2022.855052.
25. Voß, Y.; Klaus, S.; Guizetti, J.; Ganter, M. Plasmodium Schizogony, a Chronology of the Parasite's Cell Cycle in the Blood Stage. *PLOS Pathog.* **2023**, *19*, e1011157, doi:10.1371/journal.ppat.1011157.
26. Van Niekerk, D.D.; Du Toit, F.; Green, K.; Palm, D.; Snoep, J.L. A Detailed Kinetic Model of Glycolysis in Plasmodium Falciparum-Infected Red Blood Cells for Antimalarial Drug Target Identification. *J. Biol. Chem.* **2023**, *299*, 105111, doi:10.1016/j.jbc.2023.105111.
27. van Schalkwyk, D.A.; Priebe, W.; Saliba, K.J. The Inhibitory Effect of 2-Halo Derivatives of d-Glucose on Glycolysis and on the Proliferation of the Human Malaria Parasite *Plasmodium Falciparum*. *J. Pharmacol. Exp. Ther.* **2008**, *327*, 511–517, doi:10.1124/jpet.108.141929.
28. Duffy, S.; Avery, V.M. Naturally Acquired Kelch13 Mutations in Plasmodium Falciparum Strains Modulate *In Vitro* Ring-Stage Artemisinin-Based Drug Tolerance and Parasite Survival in Response to Hyperoxia. *Microbiol. Spectr.* **2022**, *10*, e01282-21, doi:10.1128/spectrum.01282-21.
29. Torrentino-Madamet, M.; Almeras, L.; Travaille; Sinou; Pophillat; Belghazi; Fourquet; Jammes; Parzy Proteomic Analysis Revealed Alterations of the Plasmodium Falciparum Metabolism Following Salicylhydroxamic Acid Exposure. *Res. Rep. Trop. Med.* **2011**, 109, doi:10.2147/RRTM.S23127.
30. Hoo, R.; Zhu, L.; Amaladoss, A.; Mok, S.; Natalang, O.; Lapp, S.A.; Hu, G.; Liew, K.; Galinski, M.R.; Bozdech, Z.; et al. Integrated Analysis of the Plasmodium Species Transcriptome. *EBioMedicine* **2016**, *7*, 255–266, doi:10.1016/j.ebiom.2016.04.011.
31. Lu, X.M.; Batugedara, G.; Lee, M.; Prudhomme, J.; Bunnik, E.M.; Le Roch, K.G. Nascent RNA Sequencing Reveals Mechanisms of Gene Regulation in the Human Malaria Parasite Plasmodium Falciparum. *Nucleic Acids Res.* **2017**, *45*, 7825–7840, doi:10.1093/nar/gkx464.
32. Bozdech, Z.; Llinás, M.; Pulliam, B.L.; Wong, E.D.; Zhu, J.; DeRisi, J.L. The Transcriptome of the Intraerythrocytic Developmental Cycle of Plasmodium Falciparum. *PLoS Biol.* **2003**, *1*, e5, doi:10.1371/journal.pbio.0000005.
33. Viscardi, M.J.; Arribere, J.A. Poly(a) Selection Introduces Bias and Undue Noise in Direct RNA-Sequencing. *BMC Genomics* **2022**, *23*, 530, doi:10.1186/s12864-022-08762-8.
34. Rang, F.J.; Kloosterman, W.P.; De Ridder, J. From Squiggle to Basepair: Computational Approaches for Improving Nanopore Sequencing Read Accuracy. *Genome Biol.* **2018**, *19*, 90, doi:10.1186/s13059-018-1462-9.
35. Kengne-Ouafo, J.A.; Bah, S.Y.; Kemp, A.; Stewart, L.; Amenga-Etego, L.; Deitsch, K.W.; Rayner, J.C.; Billker, O.; Binka, F.N.; Sutherland, C.J.; et al. The Global Transcriptome of *Plasmodium Falciparum* Mid-Stage Gametocytes (Stages II–IV) Appears Largely Conserved and Gametocyte-Specific Gene Expression Patterns Vary in Clinical Isolates. *Microbiol. Spectr.* **2023**, e03820-22, doi:10.1128/spectrum.03820-22.
36. Lee, V.V.; Judd, L.M.; Jex, A.R.; Holt, K.E.; Tonkin, C.J.; Ralph, S.A. Direct Nanopore Sequencing of mRNA Reveals Landscape of Transcript Isoforms in Apicomplexan Parasites. *mSystems* **2021**, *6*, e01081-20, doi:10.1128/mSystems.01081-20.
37. Leonardi, T.; Leger, A. Nanopore RNA Sequencing Analysis. In *RNA Bioinformatics*; Picardi, E., Ed.; Methods in Molecular Biology; Springer US: New York, NY, 2021; Vol. 2284, pp. 569–578 ISBN 978-1-07-161306-1.
38. Batugedara, G.; Lu, X.M.; Hristov, B.; Abel, S.; Chahine, Z.; Hollin, T.; Williams, D.; Wang, T.; Cort, A.; Lenz, T.; et al. Novel Insights into the Role of Long Non-Coding RNA in the Human Malaria Parasite, Plasmodium Falciparum. *Nat. Commun.* **2023**, *14*, 5086, doi:10.1038/s41467-023-40883-w.
39. Maróti, Z.; Tombácz, D.; Moldován, N.; Torma, G.; Jefferson, V.A.; Csabai, Z.; Gulyás, G.; Dörmő, Á.; Boldogkői, M.; Kalmár, T.; et al. Time Course Profiling of Host Cell Response to Herpesvirus Infection Using Nanopore and Synthetic Long-Read Transcriptome Sequencing. *Sci. Rep.* **2021**, *11*, 14219, doi:10.1038/s41598-021-93142-7.
40. Trager, W.; Jensen, J.B. Human Malaria Parasites in Continuous Culture. *Science* **1976**, *193*, 673–675, doi:10.1126/science.781840.
41. Radfar, A.; Méndez, D.; Moneriz, C.; Linares, M.; Marín-García, P.; Puyet, A.; Diez, A.; Bautista, J.M. Synchronous Culture of Plasmodium Falciparum at High Parasitemia Levels. *Nat. Protoc.* **2009**, *4*, 1899–1915, doi:10.1038/nprot.2009.198.
42. Batut, B.; Freeberg, M.; Heydarian, M.; Erxleben, A.; Videm, P.; Blank, C.; Doyle, M.; Soranzo, N.; van Heusden, P.; Delisle, L. Reference-Based RNA-Seq Data Analysis (Galaxy Training Materials) 2023a.
43. Lansink, L.I.M.; Skinner, O.P.; Engel, J.A.; Lee, H.J.; Soon, M.S.F.; Williams, C.G.; SheelaNair, A.; Pernold, C.P.S.; Laohamonthonkul, P.; Akter, J.; et al. Systemic Host Inflammation Induces Stage-Specific

Transcriptomic Modification and Slower Maturation in Malaria Parasites. *mBio* **2023**, e01129-23, doi:10.1128/mbio.01129-23.